U.S. Department of the Interior
Geological Survey

Estimation of the sensitivity of CSEM coupling to Coil Movement and Resistivity Changes of Simple Models

by

Jim Kauahikaua

Open-File Report 84-645

1984

INTRODUCTION

Beginning in March 1979, the mutual coupling between a single, large, horizontal, loop source and several vertical-axis sensor coils has been measured at approximately regular intervals in order to monitor changes in the subsurface resistivity at Kilauea volcano, Hawai'i that may be related to volcanic processes (Jackson and others, 1984). Because Kilauea inflates and deflates with a considerable amplitude of ground deformation and because the source and sensor loops are mounted in or on the ground, it is possible that the ground movement can also cause changes in the measured mutual coupling. One purpose of this report is to calculate the magnitude of the change produced by physical movement of the sensor coil with respect to the source loop.

The second purpose of this report is to examine several aspects of mutual coupling changes produced by simple resistivity changes using two simple theoretical earth models. First, changes in a horizontally-layered halfspace model show the effects of a laterally-uniform resistivity change within a limited depth interval. Second, lateral changes in the conductance of a single thin sheet approximate the effects of a spatially-limited resistivity change within a limited depth interval. The results of this modelling will aid interpretion of the changes in coupling reported by Jackson and others (1984).

The Effects of Coil Movement

Because the coils are either buried in the ground or are laid out on the ground surface, they move with the ground and with respect to each other as Kilauea volcano inflates and deflates through its normal eruption or intrusion cycle (see, for example, Jackson and others, 1975). The ground surface can translate as much as a meter vertically or horizontally and can tilt or rotate several hundred microradians. It is important to estimate how large the changes in mutual coupling due to this movement might be.

The primary effects of vertical and lateral translation will be calculated from the spatial derivatives of the primary field

of a vertical magnetic dipole (VMD) source. The secondary fields also vary spatially, but at a much slower rate so the change of the total field is almost wholly equal to the change in the primary field alone. The primary field (Wait, 1982, p. 113) and its normalized derivatives are

$$H_{z0} = (IdA/4*PI) * [3*z^2/R^5 - 1/R^3]$$

$$(1/H_{z0})(dH_{z0}/dr) = (3*r*R^2 - 15*r*z^2)/(3*(zR)^2 - R^4)$$

$$(1/H_{z0})(dH_{z0}/dz) = (9*z*R^2 - 15*z^3)/(3*(zR)^2 - R^4)$$

where IdA is the VMD moment in Amps-m^2,
PI = 3.1415927,
z is the vertical distance between source and sensor,
r is the horizontal distance between source and sensor,
$R^2 = r^2 + z^2$, and
* denotes multiplication.

After substituting appropriate r and z values for each of four sensor coil locations (from Kauahikaua and others, 1983), the normalized derivatives are found not to exceed 0.003 percent per meter of vertical or 0.06 percent per meter of lateral translation. Particular values for each of the four sensor locations at Pu'u Koa'e (PUK), Puhimau (PUH), Outlet Vault (OTL), and Keanakako'i (KKK) are tabulated in Table I.

Table I. Effects of Coil Translation

site	r, m	z, m	$(1/H_{z0})(dH_{z0}/dz)$	$(1/H_{z0})(dH_{z0}/dr)$
PUK	8013	232	-.003 %/m	- .037 %/m
PUH	9609	113	-.001	- .031
OTL	5273	107	-.003	- .057
KKK	5557	61	-.002	- .054

The second type of coil movement which may induce changes in the mutual coupling is coil rotation. For a rotation from vertical through angle, b, the change may be calculated as

$$[1/H_z][\cos(b)*H_z + \sin(b)*H_r] - 1$$

where H_z and H_r denote complex quantities.

Because angle b is very small, cos(b) -> 1 and sin(b) -> b to a good approximation, and the change becomes

$$b*H_r / H_z$$

The complex ratio of horizontal to vertical field components measured over the summit area of Kilauea volcano was found not to exceed a value of 5 in magnitude and 150 degrees in phase at any frequency between .04 and 8 Hz (Kauahikaua and others, 1983). Therefore the change produced by rotation of the coil will not exceed $(100*10^{-6})*5$ or 0.05 percent in magnitude or .015 degrees in phase per 100 microradians.

The above analysis is appropriate only for relatively slow movement; however, Kilauea volcano is seismically active and the vibration of the ground during passage of a ground tremor can also induce a signal in the receiving coils. According to Faraday's law,

$$EMF = -d(flux)/dt$$

where EMF is electromotive force, and
d(flux)/dt is the rate of change of magnetic flux through the sensor coil.

In other words, if the ground movement changes the magnetic flux through the receiver coil, then a voltage will be generated in the coil by that movement. The magnetic flux will be changed by oscillatory ground movement if 1) there is a rotational component to the motion, or 2) if there is a large enough magnetic field gradient (generated by the source loop or the earth's magnetic field) in the direction of movement. For a given magnitude gradient, Faraday's law states that faster

movement will produce larger voltage changes than slower movement.

Although mutual coupling changes induced by ground oscillation can be large, they will have only a small transient effect unless the oscillation is sustained at one of the monitored frequencies. The electronics system used to measure the mutual coupling employs synchronous detection to achieve a very narrow pass band around each of the measured frequencies (Cooke and others, 1981) and oscillations at frequencies more than a fraction of a cycle/sec different from one of the monitored frequencies are almost completely filtered out. At worst, ground oscillations would produce transient fluctuations in the observed coupling and would be most likely averaged out.

The Effect of simple resistivity changes

The first model considered is that of a horizontally-layered halfspace where each layer is laterally homogeneous and uniform. Mutual coupling changes produced by resistivity changes in this model are estimated by computing two models, each with identical parameters except for the resistivity of one layer. The difference in coupling computed for the two models is taken to be the effect of the change in resistivity in the one layer.

The model parameters were taken from a least-squares fit of the measured data at the Keanakako'i location (sounding number 25 in Kauahikaua and others, 1984). The model consists of 6 layers of approximately constant thickness and has the following parameters:

Table II. Keanakako'i model

layer	resistivity, ohm-m	thickness, m
1	1000	350
2	28	400
3	28	400
4	28	450
5	3.9	450
6	1000	

Figures 1a and 1b show the amplitude and phase changes of the mutual coupling produced by a 10 percent decrease in the

resistivity of five of the six layers for a loop separation of 5500 m. Resistivity changes in layer 1 did not produce any significant mutual coupling changes and were not included in the figures. Figures 2a and 2b show the same model changes for a loop separation of 9000 m. The frequency range in each figure is .1 to 10 Hz which brackets the frequencies monitored regularly at Kilauea. Mutual coupling changes for single-layer resistivity changes of 1 percent were found to be approximately .1 of those changes computed for 10 percent resistivity changes; therefore, the effects of resistivity changes smaller than $\pm$10 percent can be interpolated from Figures 1a and 1b.

Amplitude changes by up to 6 percent and phase changes up to 2 degrees may be produced by a 10 percent decrease in an approximately 400 m thick depth interval. The largest coupling changes are produced by resistivity decreases in layers 2, 3, and 5 for the 5500 m separation and layers 2 and 5 for the 9000 m separation. Changes in layer 5 (depth of 1600 to 2050 m) are more prominent at loop separations of 9000 m than at 5500 m.

More interesting than the magnitude of these changes are the shapes of the curves with respect to frequency. The frequency at which maximum amplitude change occurs appears to be related to the depth of the resistivity change. Low peak frequencies correspond to deeper resistivity changes. The phase-change curves are also shifted to lower frequencies for deeper changes. For example, resistivity changes in layers 2 and 3 produce the largest coupling changes at a peak frequency of 10 Hz or higher, while resistivity changes in layer 5 produce the largest coupling changes at about 1.6 Hz. Such characteristics might be used to identify depth-confined but laterally unlimited resistivity changes using multi-frequency observations.

The second model considered is a single, very thin sheet with a conductance of 100 mhos representing layer 5 in the above 6-layer model at a depth of 1800 m. The time-domain response of this type of model has been thoroughly analyzed by Sidorov and Gubatenko (1974) who have estimated the contribution to the observed magnetic field of induced currents in the sheet as a function of the current's lateral location in the sheet. For this report, the time-domain response is used, but for times approximately equivalent to frequencies 5.62, 1, and .1 Hz (frequency = 1/[2 * PI * time]).

Figures 3, 4, and 5 are the fractional contribution of induced currents in the sheet to the magnetic field observed at the sensor loop 5500 m from the source loop in units m^{-2}. Figures 6, 7, and 8 show the fractional contributions for a loop separation of 9000 m. In each figure, the upper map represents the vertical magnetic field and the lower map represents the radial magnetic field. For example, in Figure 3 (time=.0283

sec), the largest contribution for the vertical field is about
2 4 2
-3.05e-6/m ; in other words, an area of 10 m contributes a magnetic field that is about 3 percent of the total observed field, but with the opposite polarity as the observed field. If the resistivity of this same area decreases by, say, 10 percent, then to a first approximation (assume no significant change in the electric fields), the currents that flow in that area generate 10 percent more magnetic field than in the original case, or the observed field at the sensor loop decreases by 0.3 percent. An identical resistivity change involving the same area but at a different location would produce a smaller change in the observed field.

As noted by Sidorov and Gubatenko, the observed magnetic field at the sensor is largely contributed by the area around the source loop at early times or high frequencies, and by the area around the sensor loop at late times or low frequencies. This behavior is apparently opposite to the behavior of VLF (Very Low Frequency) or certain AMT (Audio-MagnetoTelluric) measurements which can be considered high frequency, but depend principally on the electrical properties of the earth near the receiver. This paradox can be resolved by review of the physics of electromagnetic (EM) propagation from discrete sources on conducting halfspaces (e.g. Kraichman, 1970). EM propagation away from a discrete source travels along two different paths - through the conductive earth and through the air. For distances less than a free space wavelength, both paths are important and the results of Sidorov and Gubatenko address this case. For distances greater than a free space wavelength (the far-field or wave zone), only the path through the air is important and propagation into the earth is vertically down. VLF and AMT measurements are usually made under these latter conditions and, as such, are primarily sensitive to the electrical properties near the receiver.

The maps in Figures 3 through 8 can be used to indicate where a given source/sensor loop pair is most sensitive laterally. For a multi-sensor loop array, these maps might be overlain and used to locate a resistivity change using the coupling change magnitudes from two or more sensor loops.

Conclusions

Changes in mutual coupling observed by Jackson and others (1984) sometimes exceed one percent. From the calculations

within this report, each of the following is capable of producing an amplitude change of approximately one percent:

1. lateral translation of about 17 m,
2. vertical translation of about 333 m,
3. rotation from vertical of 2000 microradians, or 0.11 degrees,
4. at least a 1.25 percent laterally-unlimited decrease in resistivity within a depth interval of about 400 m, or
5. at least a 30 percent change in resistivity over a 10^4 m^2 area within the depth interval 1600-2000 m.

Because lateral and vertical translation and rotation (in the form of ground tilt) are measured regularly at Kilauea (e.g. Swanson and others, 1976), we may be certain that lateral or vertical translations of the above amounts have not been measured. During the monitoring period covered in Jackson and others (1984), ground tilts rarely exceeded 100 microradians. Although both these phenomena occur at Kilauea, we have demonstrated that they are responsible for minor, probably imperceptible changes in the mutual coupling monitored at Kilauea.

On the other hand, fairly small resistivity changes can cause measurable changes in the mutual coupling. A major factor causing subsurface resistivity changes at Kilauea is temperature (Kauahikaua, 1982). Below about 200 degrees C, resistivity of water-saturated rocks decrease by an average of 0.5 percent per degree C (the average rate is quoted here because the decrease is actually exponential). Between approximately 200 and 400 degrees C, resistivity doesn't vary much with temperature change. Between 400 and 600 degrees C, resistivity *increases* by an average of 0.5 percent per degree C. Above 600 degrees C, resistivity again *decreases* by an average 0.5 percent per degree C. The above average rates are graphically estimated from composite resistivity versus temperature curves in Kauahikaua and others (1984). They should only be used as an indicator of order of magnitude change within a given temperature range.

If we assume that the primary factor causing resistivity changes at Kilauea is temperature, then a 1 percent change in the mutual coupling can be produced by a 2.5 degrees C laterally uniform change in temperature between 1600 and 2050 m depth or a laterally-limited temperature change of over 60 degrees within a $10,000$ m^2 area in the same depth range.

REFERENCES

Cooke, J., Bradley, J., Mitchell, C. and Lescelius, R., 1981, A description of an extremely low-frequency loop-loop geophysical system: U.S. Geological Survey Open-File Report 81-1130, 64 p.

Jackson, D.B., Swanson, D.A., Koyanagi, R.Y., and Wright, T.L., 1975, The August and October 1968 East Rift Eruptions of Kilauea Volcano, Hawaii: U.S. Geological Survey Professional Paper 890, 33 p.

Jackson, D.B., Kauahikaua, J., and Zablocki, C.J., 1984, Resistivity Monitoring of an active volcano using the controlled-source electromagnetic technique - Kilauea, Hawaii: submitted to Journal of Geophysical Research.

Kauahikaua, J., 1982, The subsurface resistivity structure of Kilauea volcano, Hawai'i: Ph.D. dissertation, Dept. of Geology and Geophysics, Univ. of Hawaii, 189 p.

Kauahikaua, J., Jackson, D.B., and Zablocki, C.J., 1983, Complete data listings for CSEM soundings on Kilauea Volcano, Hawai'i: U.S. Geological Survey Open-File Report 83-66, 49 p.

Kraichman, M.B., 1970, Handbook of electromagnetic propagation in conducting media: Government Printing Office, Washington, D.C.

Sidorov, V.A. and Gubatenko, V.P., 1974, On the resolution of electromagnetic prospecting by the build-up method: Isvestia, Earth Physics, no. 3, p. 173-176.

Swanson, D.A., Duffield, W.A., and Fiske, R.S., 1976, Displacement of the south flank of Kilauea Volcano: the result of forceful intrusion of magma into the rift zones: U.S. Geological Survey Professional Paper 963, 39 p.

Wait, James R., 1982, Geo-electromagnetism: Academic Press, New York, 268 p.

Figure 1. Changes in the mutual coupling between two horizontal, coplanar wire loops 5500 m apart resulting from decreasing the resistivity of layers 2 through 6 individually of the horizontally-layered earth model in Table II. Percent amplitude change versus log(frequency) is plotted in the upper graph while degree phase change versus log(frequency) is shown in the lower graph.

Figure 2. Changes in the mutual coupling between two horizontal, coplanar wire loops 9000 m apart resulting from decreasing the resistivity of layers 2 through 6 individually of the horizontally-layered earth model in Table II. Percent amplitude change versus log(frequency) is plotted in the upper graph while degree phase change versus log(frequency) is shown in the lower graph.

Figure 3 through 5. Fractional contributions made by currents flowing in the thin sheet to the total field measured at the receiver. Transmitter and receiver are 5500 m apart.

Figure 6 through 8. Fractional contributions made by currents flowing in the thin sheet to the total field measured at the receiver. Transmitter and receiver are 9000 m apart.

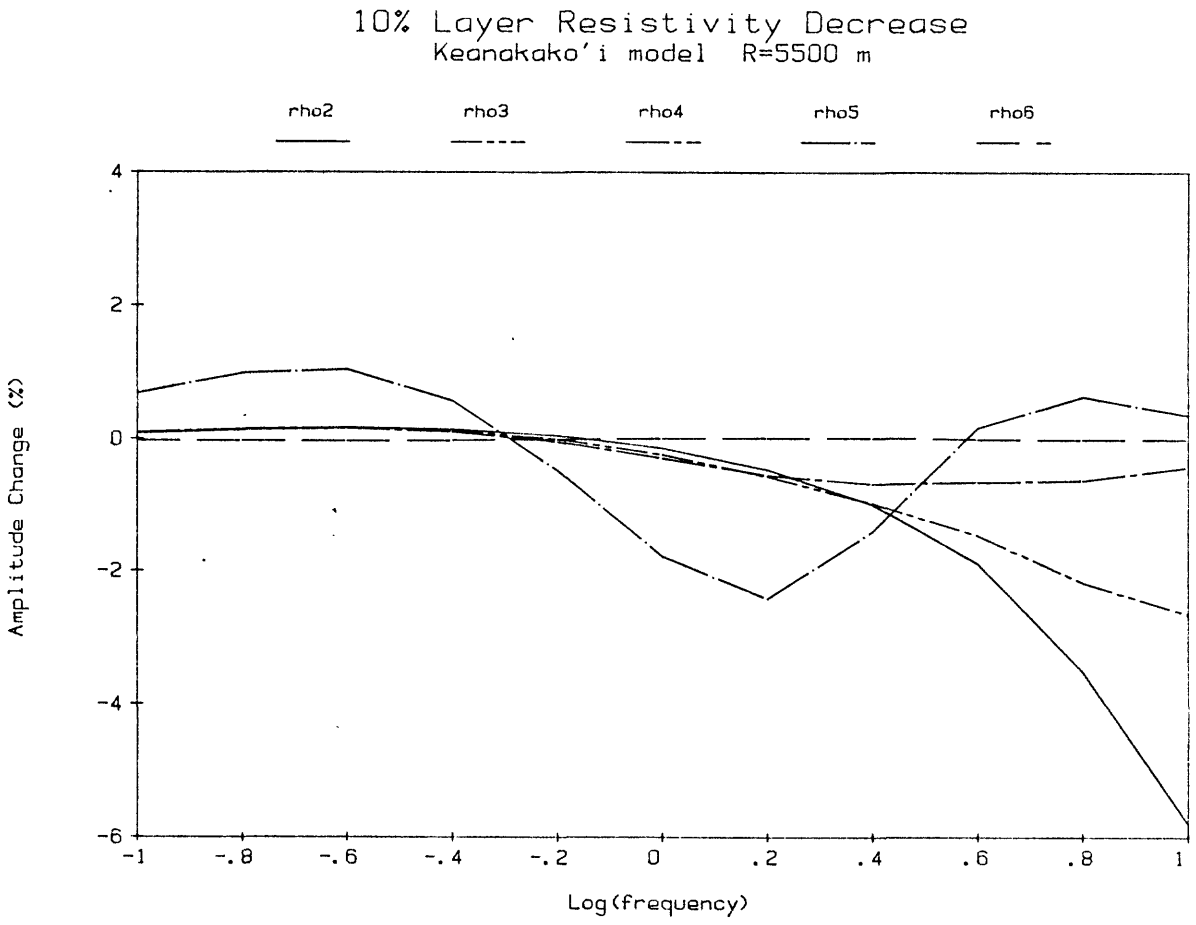

Figure 1a and 1b.

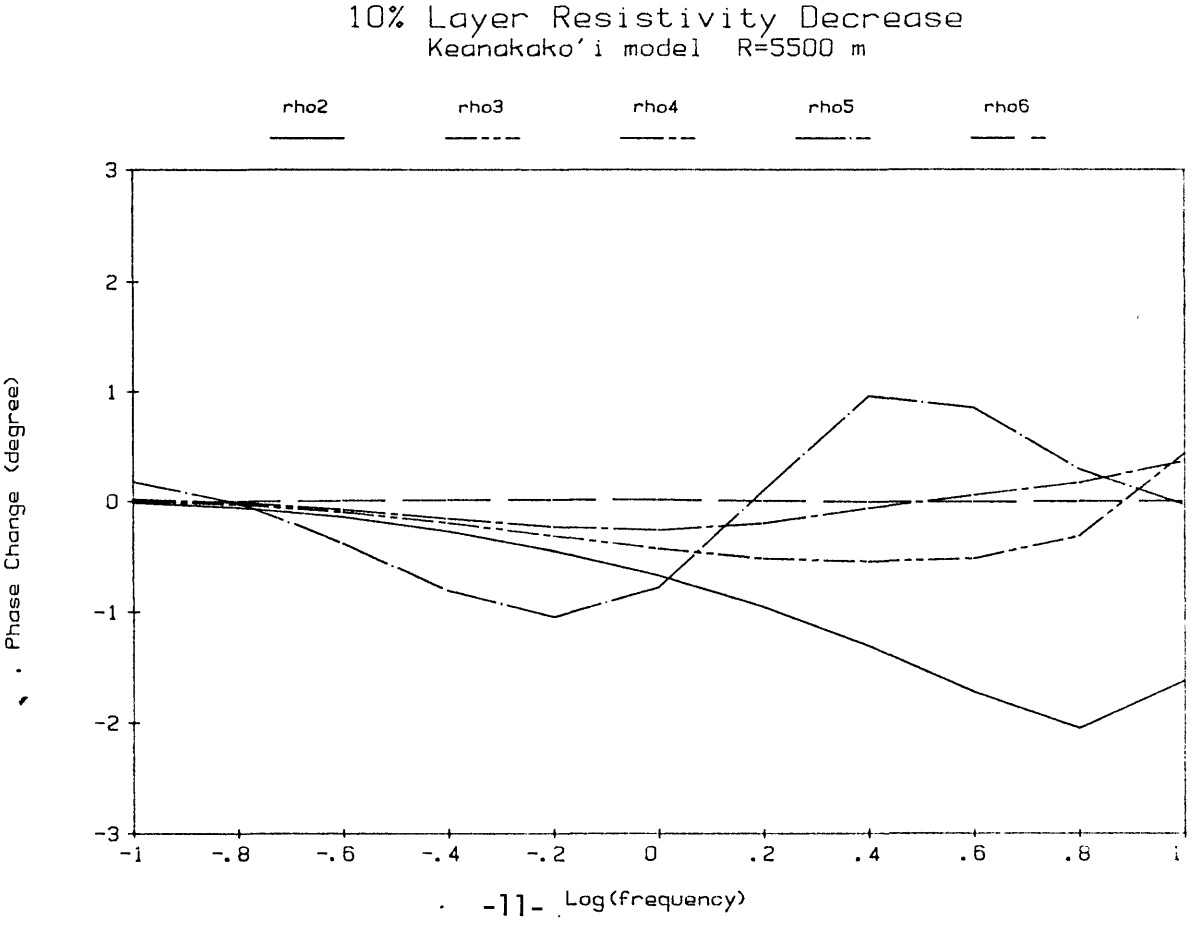

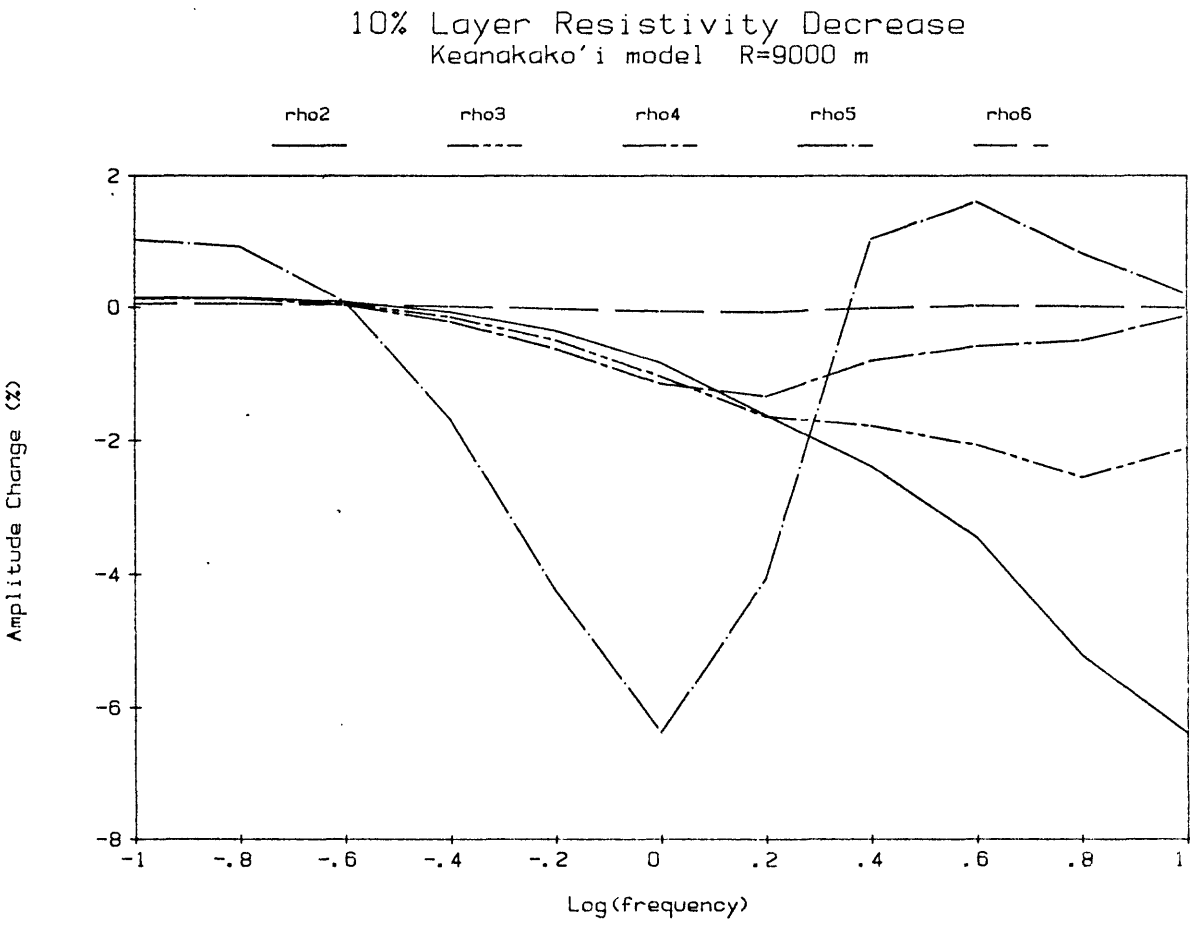

Figure 2a and 2b.

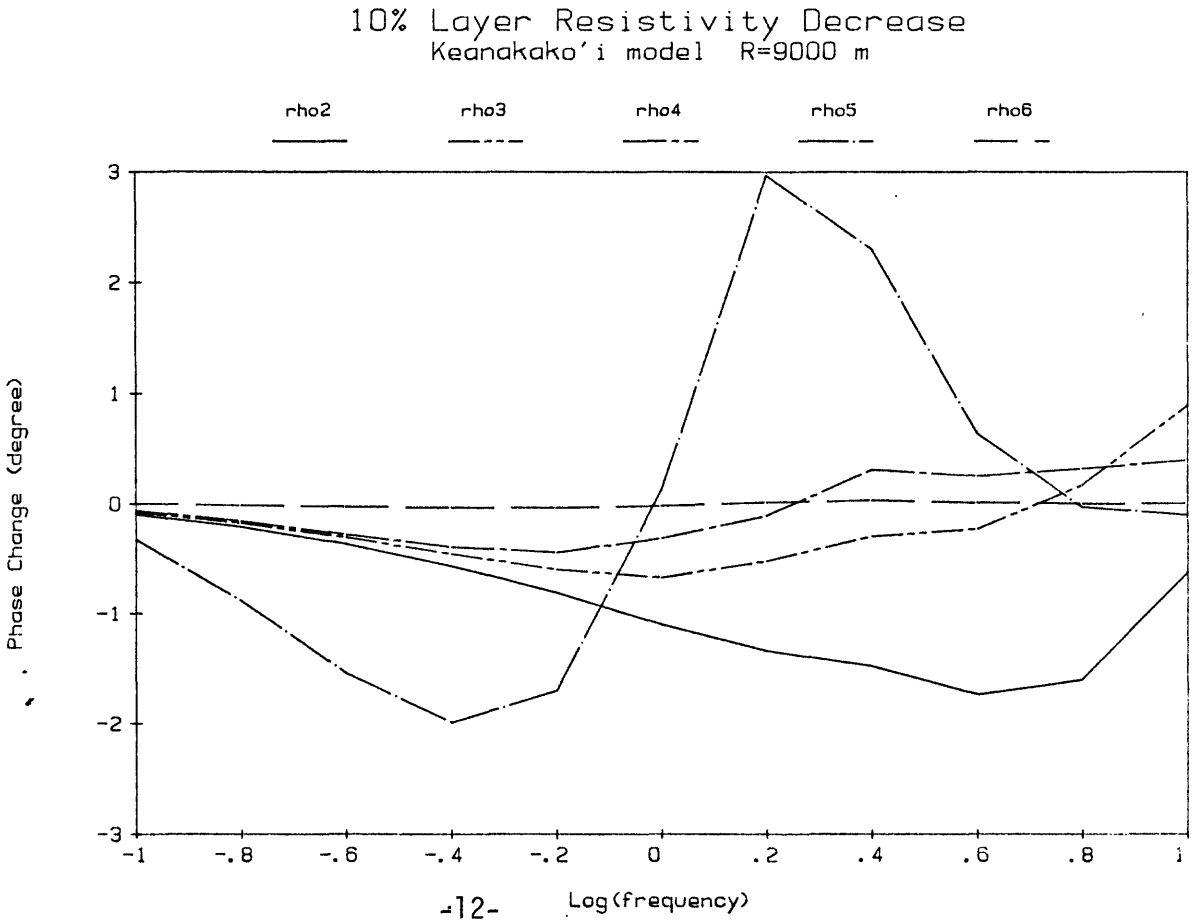

TX-RX DISTANCE=5500 H=1800 Time=.0283 CONDUCTANCE=100

FIGURE 3A: NORMALIZED VERTICAL MAGNETIC FIELD
S - SOURCE LOOP, R - RECEIVER LOOP

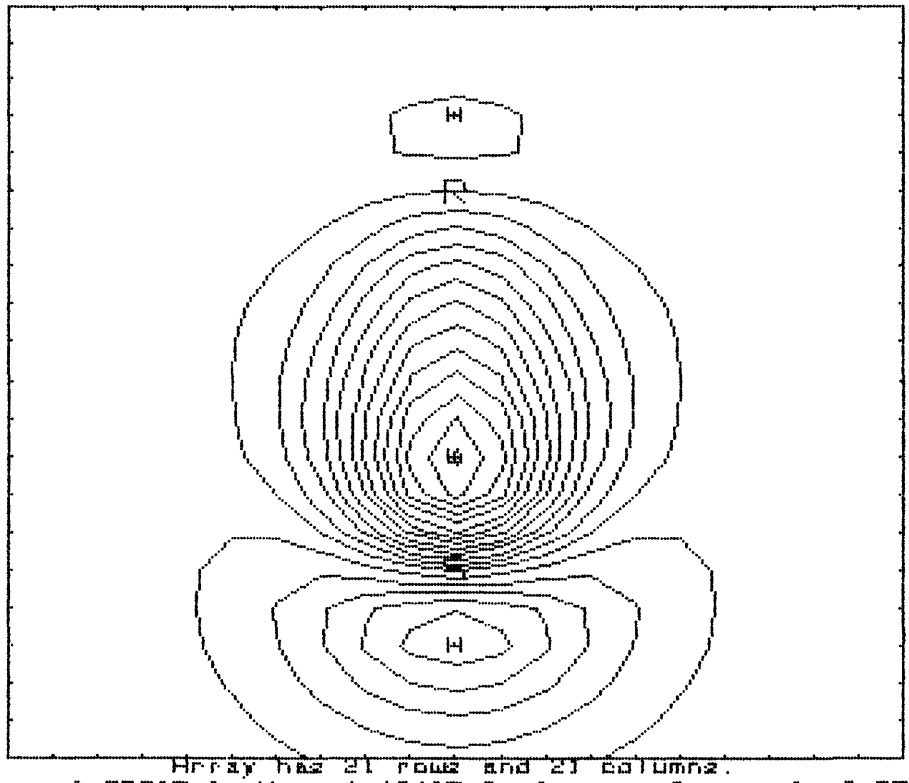

Array has 21 rows and 21 columns.
Min: -3.0502E-6; Max: 1.4342E-6; Contour Interval: 2.5E-7

FIGURE 3B: NORMALIZED RADIAL MAGNETIC FIELD
S - SOURCE LOOP, R - RECEIVER LOOP

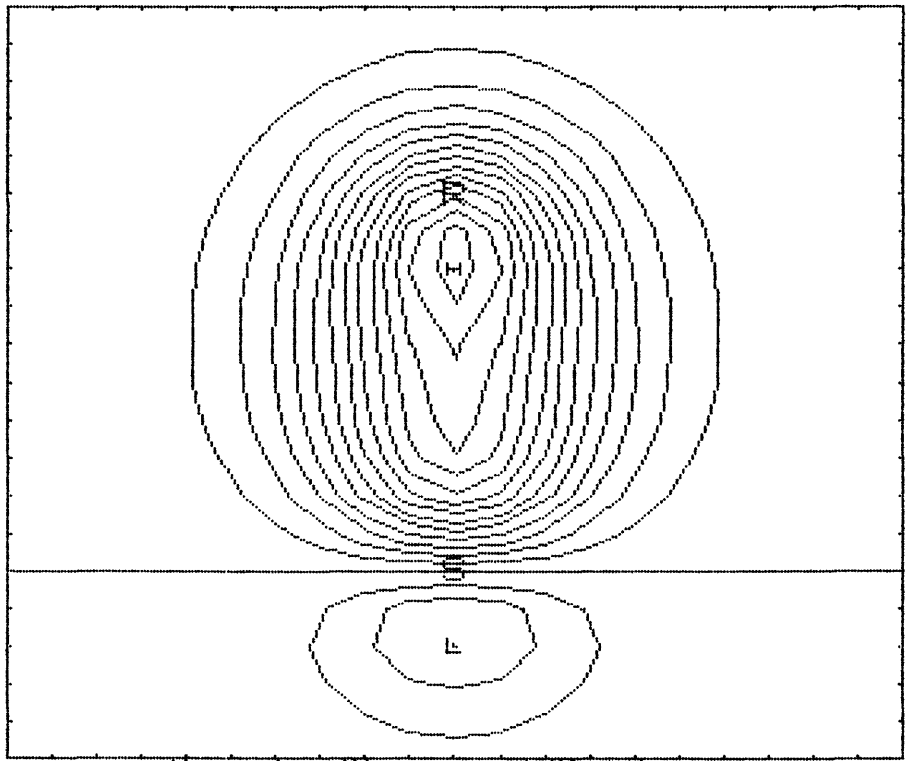

Array has 21 rows and 21 columns.
Min: -1.4992E-8; Max: 5.8409E-8; Contour Interval: 5.E-9

TX-RX DISTANCE=5500 H=1800 Time=.159 CONDUCTANCE=100

FIGURE 4A: NORMALIZED VERTICAL MAGNETIC FIELD
S - SOURCE LOOP, R - RECEIVER LOOP

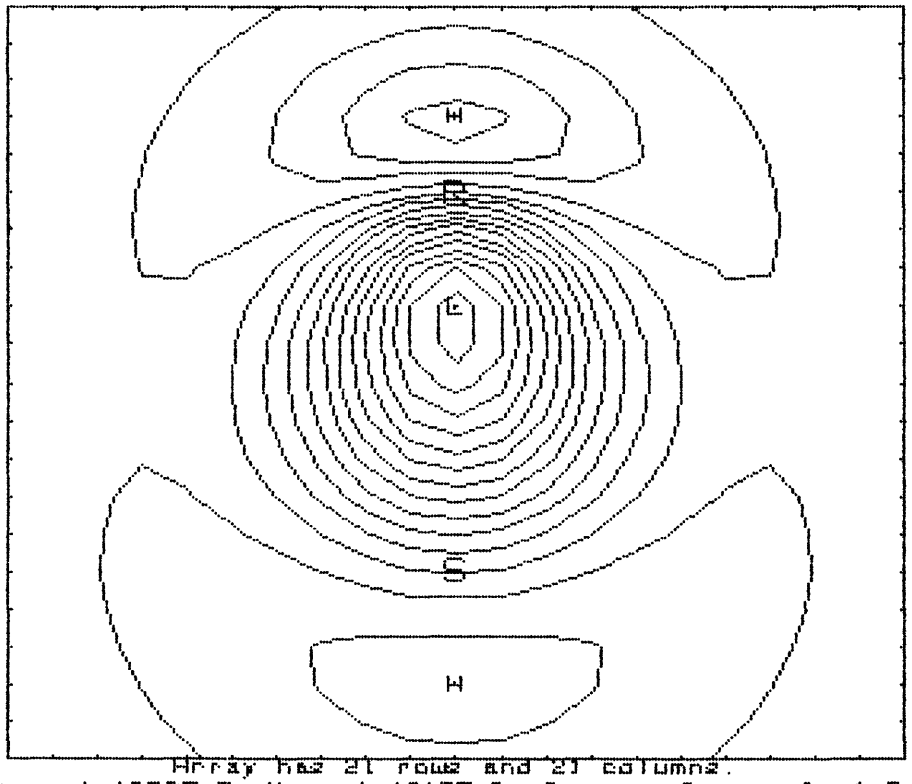

Array has 21 rows and 21 columns.
Min: -1.1652E-7; Max: 4.4017E-8; Contour Interval: 1.E-8

FIGURE 4B: NORMALIZED RADIAL MAGNETIC FIELD
S - SOURCE LOOP, R - RECEIVER LOOP

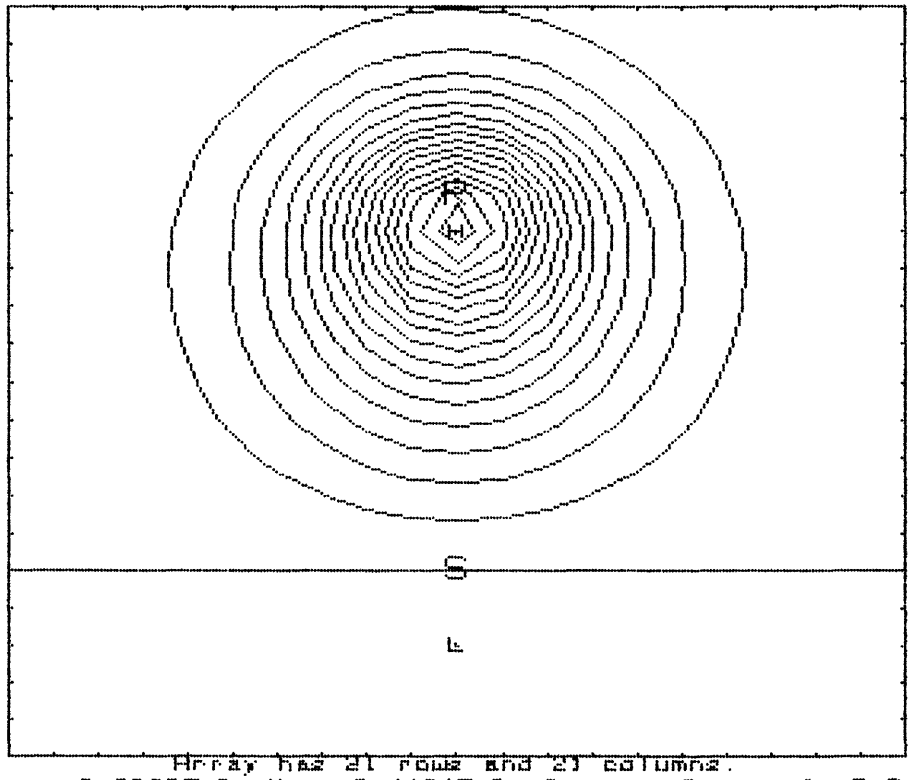

Array has 21 rows and 21 columns.
Min: -2.6909E-9; Max: 8.4121E-8; Contour Interval: 5.E-9

TX-RX DISTANCE=5500 H=1800 Time=1.59 CONDUCTANCE=100

FIGURE 5A: NORMALIZED VERTICAL MAGNETIC FIELD
S - SOURCE LOOP, R - RECEIVER LOOP

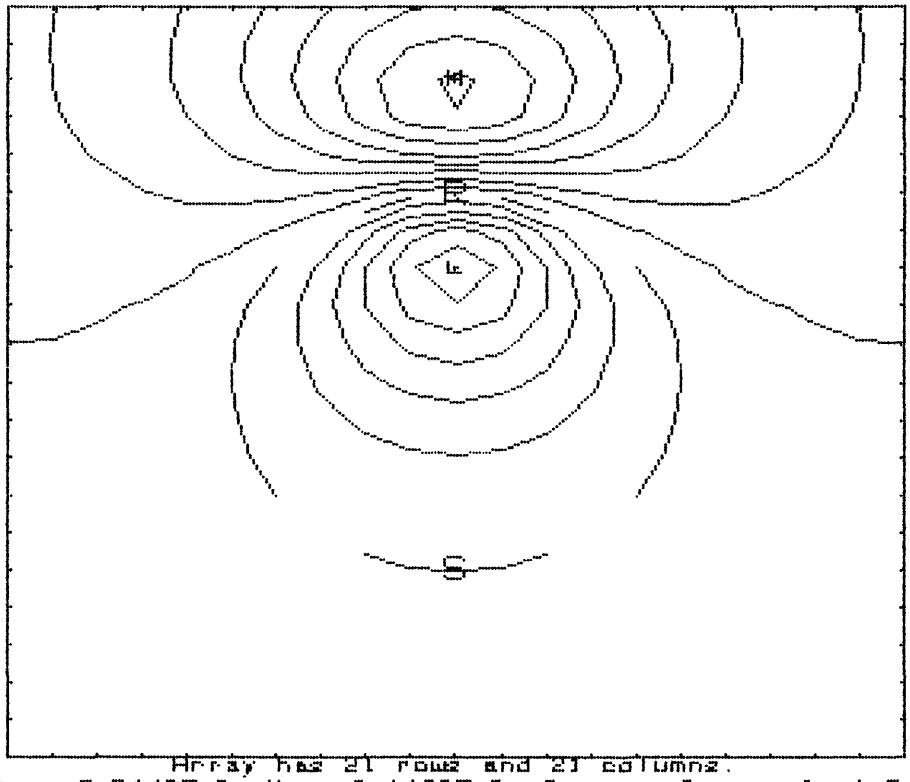

Array has 21 rows and 21 columns.
Min: -5.7443E-9; Max: 8.1429E-9; Contour Interval: 1.E-9

FIGURE 5B: NORMALIZED RADIAL MAGNETIC FIELD
S - SOURCE LOOP, R - RECEIVER LOOP

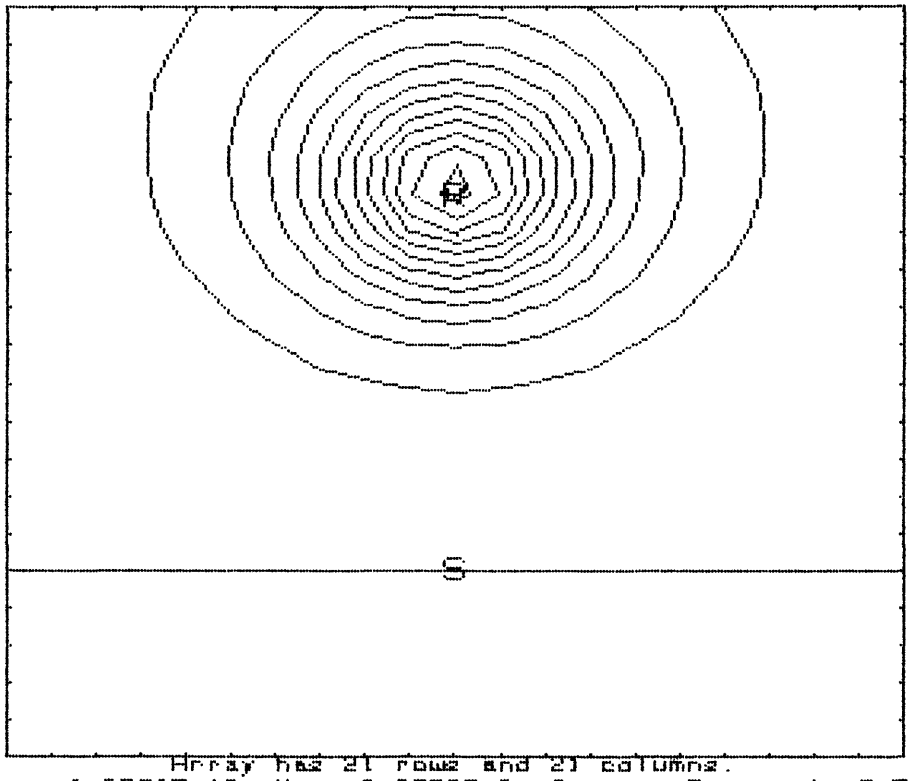

Array has 21 rows and 21 columns.
Min: -9.2729E-10; Max: 6.2773E-8; Contour Interval: 5.E-9

TX-RX DISTANCE=9000 H=1800 Time=.0283 CONDUCTANCE=100

FIGURE 6A: NORMALIZED VERTICAL MAGNETIC FIELD
S - SOURCE LOOP, R - RECEIVER LOOP

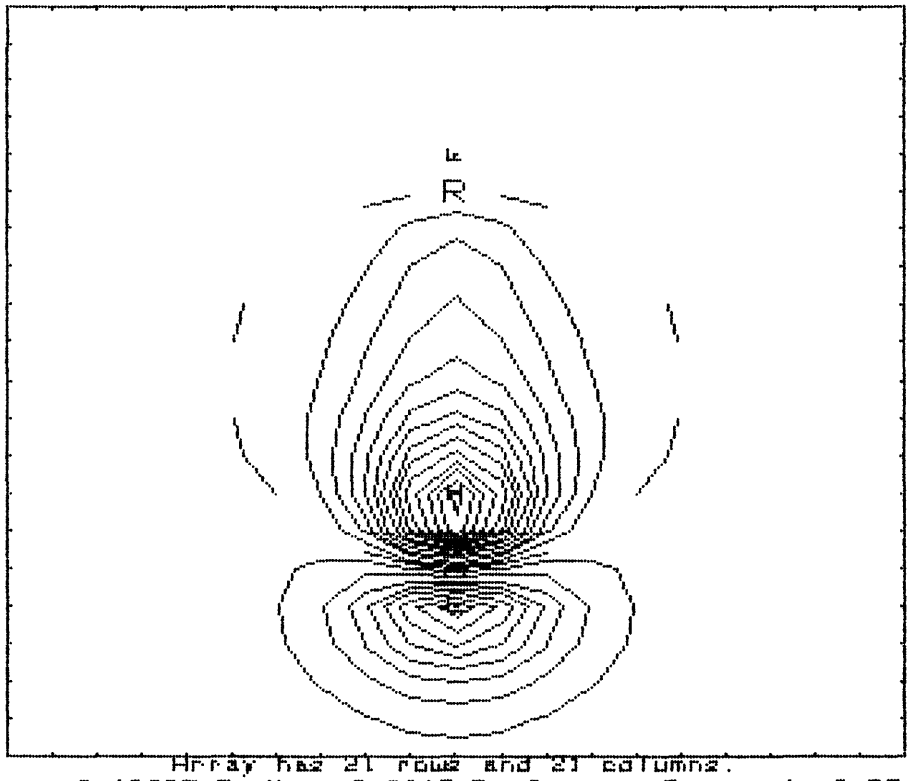

Array has 21 rows and 21 columns.
Min: -2.1833E-7; Max: 3.331E-7; Contour Interval: 2.5E-8

FIGURE 6B: NORMALIZED RADIAL MAGNETIC FIELD
S - SOURCE LOOP, R - RECEIVER LOOP

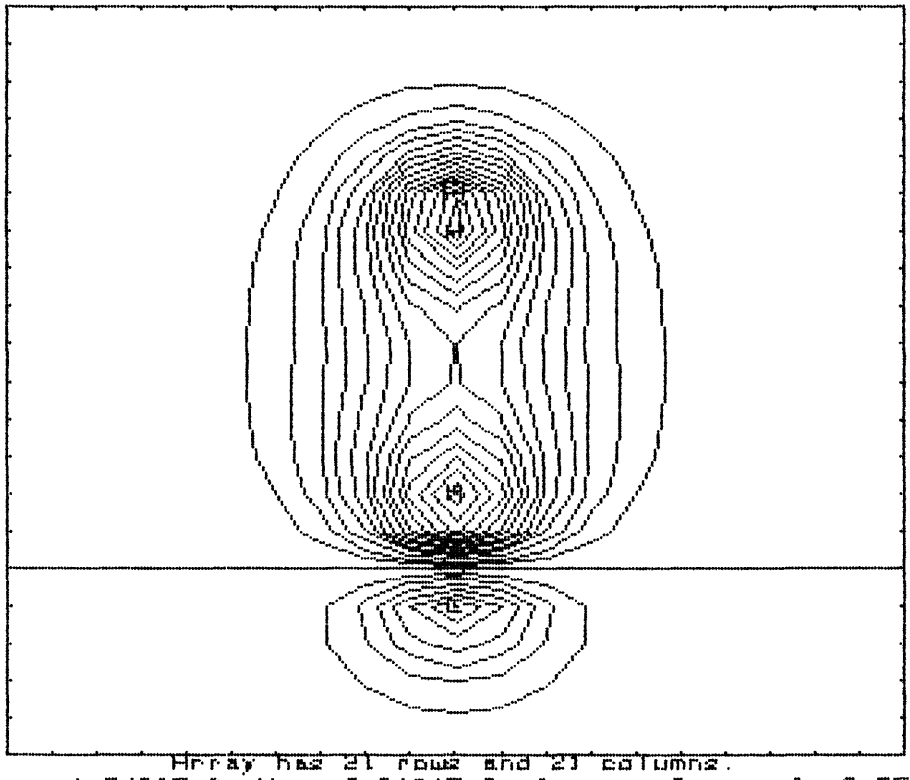

Array has 21 rows and 21 columns.
Min: -1.2492E-8; Max: 3.9194E-8; Contour Interval: 2.5E-9

TX-RX DISTANCE=9000 H=1800 Time=.159 CONDUCTANCE=100

FIGURE 7A: NORMALIZED VERTICAL MAGNETIC FIELD
S - SOURCE LOOP, R - RECEIVER LOOP

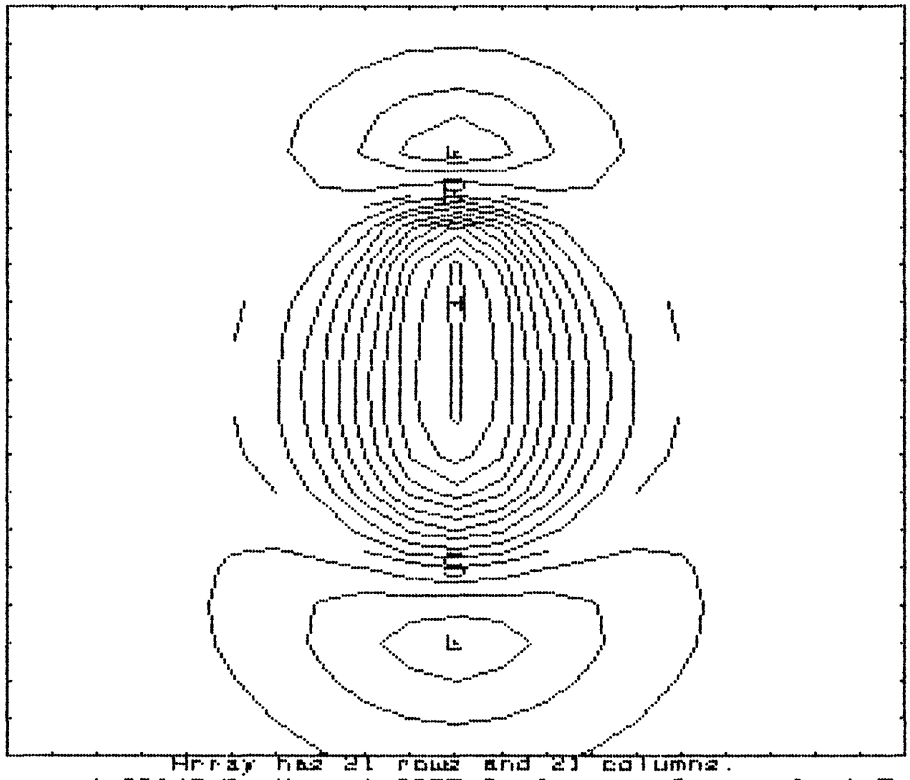

Array has 21 rows and 21 columns.
Min: -4.0284E-7; Max: 1.035E-6; Contour Interval: 1.E-7

FIGURE 7B: NORMALIZED RADIAL MAGNETIC FIELD
S - SOURCE LOOP, R - RECEIVER LOOP

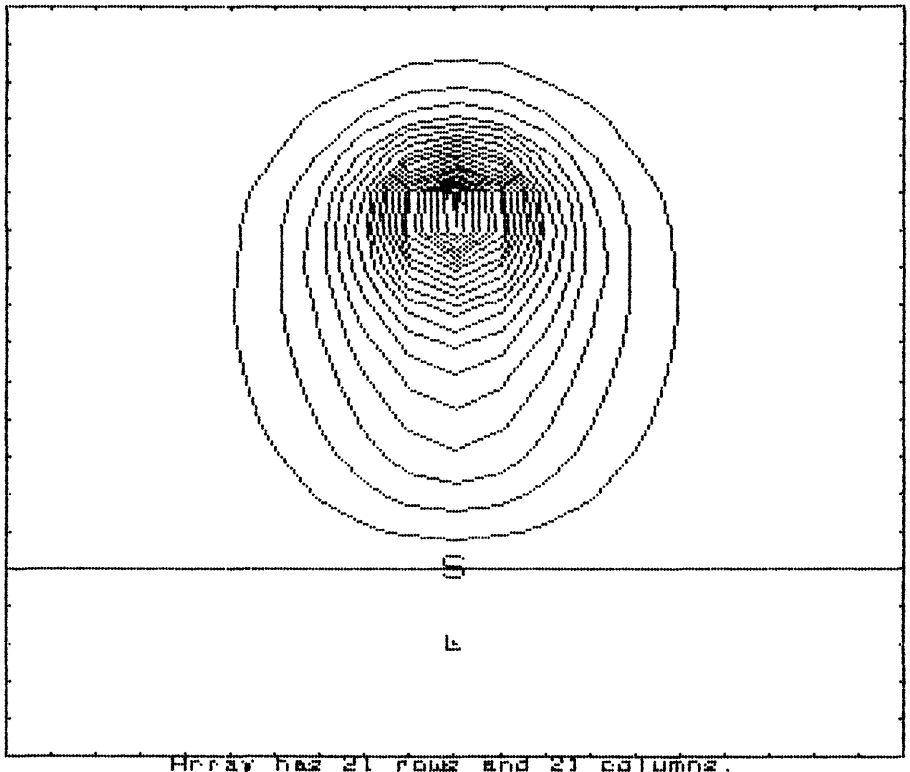

Array has 21 rows and 21 columns.
Min: -2.0814E-9; Max: 5.3464E-8; Contour Interval: 2.5E-9

TX-RX DISTANCE=9000 H=1800 Time=1.59 CONDUCTANCE=100

FIGURE 8A: NORMALIZED VERTICAL MAGNETIC FIELD
S - SOURCE LOOP, R - RECEIVER LOOP

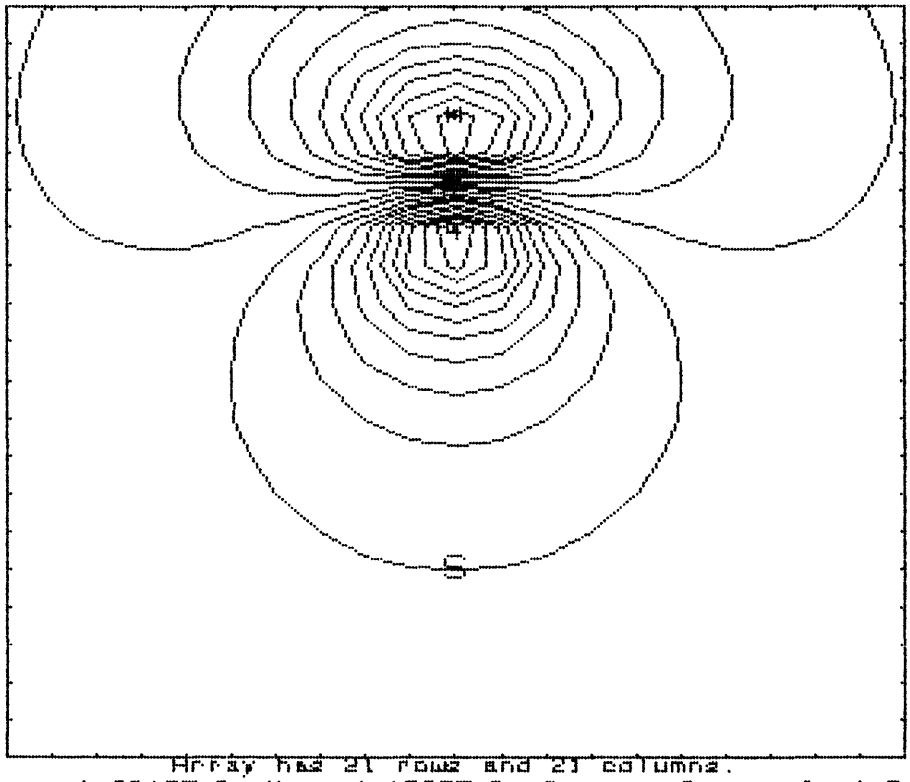

Array has 21 rows and 21 columns.
Min: -1.0217E-8; Max: 1.1535E-8; Contour Interval: 1.E-9

FIGURE 8B: NORMALIZED RADIAL MAGNETIC FIELD
S - SOURCE LOOP, R - RECEIVER LOOP

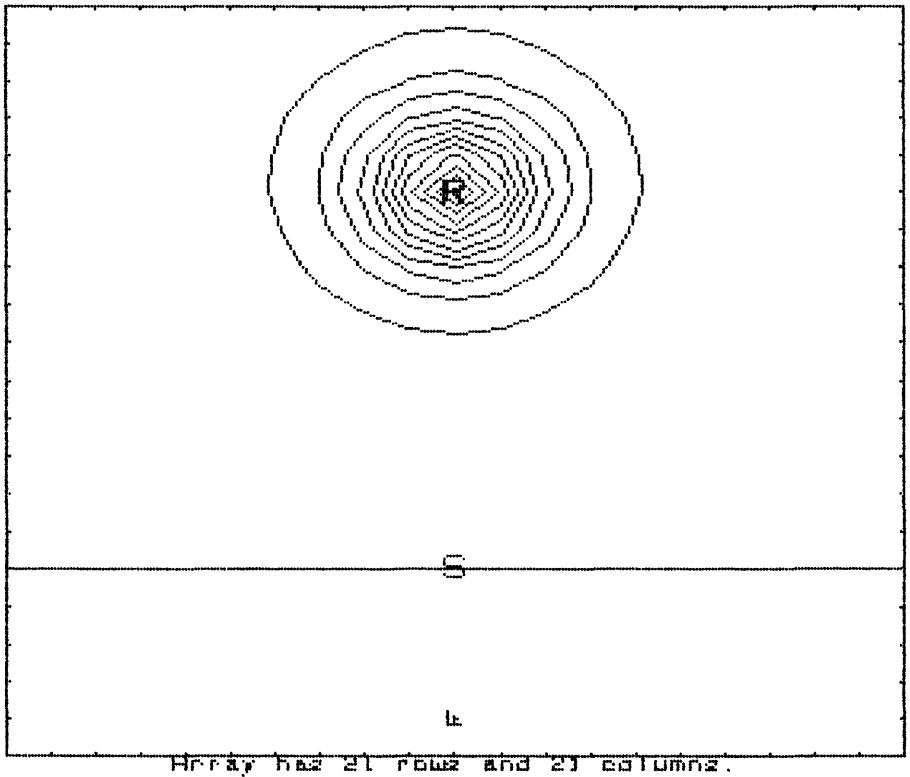

Array has 21 rows and 21 columns.
Min: -8.6706E-11; Max: 6.1642E-8; Contour Interval: 5.E-9